Impact of the Diffusion Limitation in Microphotoreactors

Tristan Aillet, Karine Loubière, and Laurent Prat
Université de Toulouse; INPT, ENSIACET, F-31432 Toulouse, France

CNRS, Laboratoire de Génie Chimique (LGC UMR 5503), 4 allée Emile Monso, BP 84234, F-31432 Toulouse, France

Odile Dechy-Cabaret
Université de Toulouse; INPT, ENSIACET, F-31432 Toulouse, France

CNRS, Laboratoire de Chimie de Coordination (LCC UPR 8241), 205 route de Narbonne, BP 44099, F-31077 Toulouse, France

DOI 10.1002/aic.14718
Published online January 10, 2015 in Wiley Online Library (wileyonlinelibrary.com)

This publication describes a model that aims (1) to predict the performances (conversion, photonic efficiency) of a photochemical reaction at the outlet of a microreactor. To achieve this, a set of equations that couple mass transport, radiative transfer, and kinetic equations is established and solved, considering (1) a two-dimensional geometry and (2) a simple monomolecular photoreaction $A \xrightarrow{h\nu} B$*, where the species A and B are in competition for absorbing incident photons. The model is expressed using classical dimensionless numbers, such as the Damköhler I and II numbers, the absorbance, and the competitive absorption factor. The results show how and why, when competitive absorption exists, the occurrence of diffusion limitations* ($Da_{II} > 1$) *can severely impact the conversion of the photochemical reaction and the photonic efficiency. Consequently, a diagram is proposed as a practical tool for selecting operating conditions subsequently avoiding these limitations.* © 2015 American Institute of Chemical Engineers *AIChE J*, 61: 1284–1299, 2015
Keywords: flow photochemistry, radiative transfer, competitive absorption, modeling, dimensionless numbers

Introduction

Photochemistry is a powerful method for the conversion of simple molecules into new and/or complex products, opening promising perspectives in particular for synthetic organic chemistry.[1,2] When compared to thermal pathways, photochemical reactions commonly occur without additional reagents, thus reducing the formation of by-products. This feature makes photochemistry attractive in the modern context of Green Chemistry.[1–3] Despite some large-scale technical applications[2,4,5] the industrial usage of preparative photochemistry is still limited due to concerns about the scalability of light sources and the difficulty of reproducing yields and selectivities when transferring from the laboratory scale to the industrial one. Over the last decades, microreaction technology has been successfully developed to improve reaction outcomes.[6–9] For photochemistry, microreactors offer additional advantages, such as higher spatial illumination homogeneity and better light penetration.[7,10,11] A number of publications have clearly demonstrated that microphotoreactor scan, in the case of both photocatalysis[12–15] and noncatalyzed photoreactions,[16–22] enhance conversions and selectivities, reduce irradiation time and improve productivities and space-time yields. Despite these promising findings, there are currently only a few reports that try to understand and model the positive effects of microspace on reaction performances from a reaction engineering perspective. We have previously reported the first papers for noncatalyzed photochemical transformations like the ones described in this work.[23,24] This research gap is all the more surprising as:

- previous studies[25,26] have determined the kinetic constants of a photocatalytic reaction, and more generally, modeled the photocatalytic efficiency in microreactors, by taking into account mass-transfer limitations;
- for several decades, the theory of photoreactor engineering has been defined by rigorously deriving reaction engineering principles and radiative energy transport fundamentals[27–32];
- and more recently, 3-D numerical simulations (using a commercial CFD package) have been implemented to predict the (radical) photochemical degradation of pollutants in large-scale photoreactors, in particular for water/air treatment applications.[33–35]

In this context, this work aims to apply a reaction engineering methodology for modeling the conversion of noncatalyzed organic photochemical reactions inside microreactors. The ultimate objective is to define the relevant criteria that enable a transfer of photochemical synthesis from batch to continuous flow photoreactors (including microreactors). A set of equations describing the conversion profile along the

Additional Supporting Information may be found in the online version of this article.

Correspondence concerning this article should be addressed to K. Loubière at Karine.Loubiere@ensiacet.fr.

Corrections added on 28 January 2015, after first online publication.

microreactor length will be subsequently established and numerically solved considering a two-dimensional (2-D) geometry and a cartesian coordinate system (first section). By nondimensionalization of the set of equations to solve, various dimensionless numbers will be highlighted (second section). This article will focus on the influence of the Damköhler II number (Da_{II}), which compares the photochemical reaction rate with the mass diffusion rate along the light path length (third section). For this study, a simple monomolecular reaction $A \xrightarrow{h\nu} B$ where the species A and B are in competition for absorbing incident photons will be considered as a benchmark noncatalyzed photoreaction. This general reaction pathway is commonly encountered in preparative photochemistry, for example, in the phototransformation of ergosterol to produce previtamin D2 or in the photoisomerization of the humulone α-acid to iso-humulone[28] (for additional examples, see Ref. 1). In the last section, the methodology developed will establish some practical guidelines for selecting the operation conditions to avoid mass-transfer limitations (i.e., to ensure a plug flow reactor [PFR] behavior), and discuss, through a case study, the positive effects of photoreactor miniaturization on outcome of phototransformations.

Problem Formulation

In this section, a set of equations used to predict conversion inside continuous microphotoreactors is presented for the case of a simple photochemical transformation $A \xrightarrow{h\nu} B$. In this benchmark reaction, the species A and B are in competition for absorbing incident photons at the same wavelength λ. The photons absorbed by A lead to the production of B, the product B being considered as a photostable species. It must be noted that the model proposed in this study is specifically applied to microreactors, but it could be generally transferred to any type of continuous photoreactors (in particular at larger scale), assuming that the coordinate system and the boundary conditions are adjusted to the geometries of the photoreactor and light source.

Conventionally, the modeling of a photoreactor requires accounting for mass transport, energy conservation, momentum transport, and radiative transfer equations. Photochemical reactions are based on the use of photons to provide the activation energy required to form a target molecule. In the case of a strictly photochemical reaction (i.e., a reaction where the desired product is formed only from photon absorption), the effect of temperature can be neglected as the temperature dependency of photon absorption process is negligible.[3,36] Consequently, photochemical kinetics can be decoupled from the temperature field. For this reason, and with respect to the reaction scheme chosen, this study does not take into account temperature variations inside the reactor. Thus, microreactors will be assumed operating at ambient temperature and the energy conservation equation will not be solved.

Geometrical considerations and mass balance equation

The main features of a continuous microphotoreactor are: (1) its characteristic dimension with respect to the light penetration direction (i.e., the diameter or width of the microreactor), which is by definition of micrometric magnitude and (2) its long length (classically ranged from several centimeters to a meter or more) used to increase residence time and productivity.

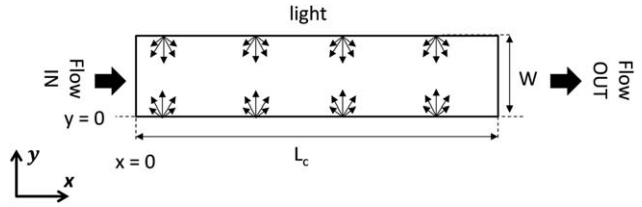

Figure 1. Coordinate system and geometrical domain adopted for the modeling of microphotoreactors.

When compared to conventional microreactors, microphotoreactors incorporate a light source, either internally or externally. One of the commonly and easily built microphotoreactor is the capillary tower reactor constructed by winding a transparent and chemically inert tube around an immersion well in which the lamp (generally a polychromatic vapor discharge mercury lamp) is inserted.[18,23,37] Other types of devices exist, for example, serpentine plate type microphotoreactoror falling film type microphotoreactor, which incorporate microchannels with a square or rectangular cross-section area illuminated from one or both sides (e.g., by a lighting-emitting diode [LED] array or a fluorescent tube panel).[20,38] From the various photoreactor configurations reported, some common features can be found: (1) the flow rates are generally in the mL min^{-1} range, and thus, the flow is laminar, (2) the reactor surfaces can be considered uniformly irradiated, and (3) the light direction can be assumed monodirectional and perpendicular to the flow direction.

In this study, the microphotoreactor will be modeled in two spatial dimensions, using a Cartesian coordinate system as shown in Figure 1. This coordinate system describes serpentine microreactors well, and is also an acceptable compromise for numerically implementing the radiative transfer equation with enough accuracy and simplicity for use. Indeed, the formulation of the radiative transfer equation in the case of a cylindrical microreactor, for which only a part of its curved optical surface is illuminated, presents a significantly higher complexity (in particular with regard to the problem of discontinuity at the center of the photoreactor). Subsequently, the microphotoreactor will be described by a rectangular domain defined by two characteristic dimensions in this study: the channel length L_c (in the x-direction, Figure 1) and a transverse dimension W (in the y-direction, Figure 1) equal to the channel width or diameter that corresponds to the thickness of the fluid irradiated.

The flow in the microreactor will be assumed steady, laminar, and fully developed. Consequently, the momentum transfer equation will be decoupled with other conservation equations and an explicit solution for the velocity field will be used, consisting in the parabolic velocity profile $u_x(y)$, where $u_x(y)$ is the axial component of the velocity and y the transverse coordinate, respectively. With regard to assumptions made to describe the microreactors (coordinate system, rectangular geometrical domain), the expression of the parabolic velocity profile obtained between two parallel plates will be considered as

$$u_x(y) = 6\bar{u}\left[\left(\frac{y}{W}\right) - \left(\frac{y}{W}\right)^2\right] \quad (1)$$

where $\bar{u}$ is the mean velocity in the microreactor. The concentration of compound A will be supposed uniform at the reactor inlet ($\boldsymbol{x}=0$) and equal to $\boldsymbol{C}_{A0}$.

Also, we will assume that:

- the radiations emitted by the light source are uniformly distributed along the reactor walls and perpendicularly to the flow direction;
- the material of the optical surfaces of the microreactor is nonreflective;
- the light source is monochromatic. This implies that all the wavelength-dependent physical quantities (e.g., absorption coefficient, quantum yield) will be calculated at a single wavelength, that is, the one emitted by the lamp. Thereafter, the subscript "λ" will be omitted to simplify equations and notations.

In addition, the following assumptions are considered: (1) axial diffusion mass flux is negligible in comparison with the convective transport of mass, (2) isothermal conditions, and (3) monophasic flow. For these conditions, the mass balance equation for reactant A is written as[39]

$$6\bar{u}\left[\left(\frac{y}{W}\right)-\left(\frac{y}{W}\right)^2\right]\frac{\mathrm{d}C_A}{\mathrm{d}x}-D_m\left(\frac{\mathrm{d}^2C_A}{\mathrm{d}y^2}\right)=-r_A \tag{2}$$

Where D_m the diffusion coefficient of the compound A and r_A the photochemical reaction rate (expressed in terms of consumption of A).

Expression of the kinetics term

Photochemical reactions are activated by light absorption. In a simple approach, the photoreaction under study, $A\xrightarrow{h\nu}B$, can, thus, be described by a three steps mechanism:

- an activation step leading to the formation of the excited species A^*,
- a deactivation step of the excited species A^*, and
- a reaction step where the compound B is produced from the excited state A^*.

The global expression of the reaction rate can be written by the following matrix equation

$$\mathbf{R}=\mathbf{M}\ \mathbf{C} \tag{3}$$

where **R**, **M**, and **C** are the matrix related to reaction rates (r_i), kinetic parameters and concentrations, respectively, as defined in Table 1.

As shown in Table 1, the activation step rate is expressed as the product of the molar napierian absorption coefficient of the species A, κ_A expressed in $\mathrm{m^2\ mol^{-1}}$, and the spherical irradiance E_o expressed in einstein $\mathrm{m^{-2}\ s^{-1}}$ (see below for definitions).

The application of the microscopic steady state approximation leads to consider no accumulation of the intermediate excited species (A*) as it is an unstable species[4]. As a result, $\frac{dC_{A*}}{dt}\approx 0$ and, therefore, C_{A*} is expressed as

$$C_{A*}=\frac{\kappa_A E_o}{k_d+k_R}C_A \tag{4}$$

The quantum yield of the photoreaction, Φ (mol einstein^{-1}), is defined, at a given wavelength, as the ratio between the rate of molar production of B and the rate of photon molar absorption

$$\Phi=\frac{r_B}{\kappa_A C_A E_o}=\frac{k_R}{k_d+k_R} \tag{5}$$

Using Eq. 3, the rate of consumption of reactant A is subsequently expressed as

Table 1. Array for the Reaction Rate Expressions

Reaction Mechanism for $A\xrightarrow{h\nu}B$			
	Activation step	$A\rightarrow A^*$	$(\kappa_A E_o)$
	Deactivation step	$A^*\rightarrow A$	(k_d)
	Reaction step	$A^*\rightarrow B$	(k_R)
Name	Symbol	Expression	
Reaction rates	**R**	$[r_A r_{A*} r_B]^T$	
Concentration	**C**	$[C_A C_{A*} C_B]^T$	
Kinetic parameters	**M**	$M=\begin{bmatrix}-\kappa_A E_o & k_d & 0\\ \kappa_A E_o & -k_d-k_R & 0\\ 0 & k_R & 0\end{bmatrix}$	

$$r_A=-r_B=\Phi\kappa_A C_A E_o \tag{6}$$

The quantity $\kappa_A C_A E_o$ (expressed in einstein $\mathrm{m^{-3}\ s^{-1}}$) is also known as the local volumetric rate of photon absorption of the compound A (LVRPA) and is noted e_A^a. Therefore, Eq. 6 is commonly written as follows

$$r_A=\Phi\ e_A^a \tag{7}$$

Expression of the spherical irradiance E_o

The complete radiative transfer equation accounting for light diffusion into a media is complex to solve because of the integrodifferential nature of the problem. Noncatalyzed photoreactions mainly deal with homogeneous media and UV radiations. Thus, this equation simplifies as light scattering and emission can be neglected. Based on these assumptions, the radiative transfer equation in a given direction **u** is written as[30,31]

$$\frac{\mathrm{d}L}{\mathrm{d}s}=-\alpha L(s,\mathbf{u}) \tag{8}$$

where L is the photon radiance (einstein $\mathrm{m^{-2}\ sr^{-1}}$), also known as the specific intensity, which represents the radiative photon flux per unit of time, unit of solid angle, and unit of surface normal to the propagation direction, and s is the curvilinear coordinate along the light path.

The linear napierian absorption coefficient, α (expressed in $\mathrm{m^{-1}}$), defined at a given wavelength, takes into account the different absorbing species present in the reaction medium. For the photochemical transformation chosen, $A\xrightarrow{h\nu}B$, it is expressed as

$$\alpha=\sum_i \kappa_i C_i=\kappa_A C_A+\kappa_B C_B \tag{9}$$

Considering Eq. 8 for all the solid angles (i.e., all the directions), the radiation balance for nonemitting and homogeneous control volume is obtained[40]

$$\mathbf{\nabla}(\mathbf{F})=-\alpha E_o \tag{10}$$

where E_o is the spherical irradiance (einstein $\mathrm{m^{-2}\ s^{-1}}$), that is, the sum of the photon radiation incoming from all the directions (the subscript "o" means overall) expressed as

$$E_o=\int_{\Omega=4\pi} L\mathrm{d}\Omega \tag{11}$$

And **F** is the photon flux density vector (einstein $\mathrm{m^{-2}\ s^{-1}}$) defined as

$$\mathbf{F}=\int_{\Omega=4\pi} L\mathbf{u}\mathrm{d}\Omega \tag{12}$$

Equation 10 is an integrodifferential equation in a six dimensional Euclidean space, which requires numerical methods to be solved.[41] To simplify the problem, the angular space is commonly divided in two main opposite directions. This latter method is called the two flux approximation, initially introduced by Schuster.[42] This method has been extended by Cornet to cylindrical and spherical geometries.[43] The solution of the radiative transfer equation is reported in Supporting Information and leads to the following set of equations

$$\begin{cases} \dfrac{\mathrm{d}E^+}{\mathrm{d}y}=-\Lambda\alpha E^+=-\Lambda(\kappa_A C_A+\kappa_B C_B)E^+ \\ \dfrac{\mathrm{d}E^-}{\mathrm{d}y}=-\Lambda\alpha E^-=\Lambda(\kappa_A C_A+\kappa_B C_B)E^- \end{cases} \tag{13}$$

where C_A and C_B are the concentrations of the reactant A and the product B, respectively, and depend on the spatial location (x,y). $E^{\pm}$ are the spherical irradiances in the two opposite directions; their sum gives the total spherical irradiance E_o, required to calculate the rate of consumption of reactant A, r_A (Eq. 7)

$$E_o=E^-+E^+ \tag{14}$$

In Eq. 13, Λ is the collimation factor[43]: if $\Lambda=1$, the radiation field is supposed collimated and if $\Lambda=2$, the radiation field is supposed isotropic (see Supporting Information).

The boundary conditions required to solve Eq. 13 are given in Supporting Information. They are defined from the photon flux density at the reactor wall F_{wall} (classically measured by actinometry[24] or by using a radiometer) and from the parameter υ introduced to account for one ($\upsilon=0$) or both ($\upsilon=1$) illuminated sides.

At last, the local volumetric rate of photon absorbed for a compound "i," e_i^a, is directly obtained from the resolution of Eq. 13

$$e_i^a=\kappa_i C_i E_o=\kappa_i C_i(E^++E^-) \tag{15}$$

When examining Eqs.13 and 15, two important conclusions can be drawn. On the one hand, the formal solution of Eq. 13 is of exponential nature. Therefore, even if the concentrations of the absorbing species are perfectly homogeneous along the radiation penetration depth in the media, the local volumetric rate of photons absorbed, e_i^a, and thus, the subsequent kinetic rate of the photoreaction r_A, will be heterogeneous along the radiation penetration. On the other hand, because the solution of Eq. 13, (E_o), used to calculate e_i^a, depends on the local concentration fields, Eqs. 2 and 13 are coupled together via the kinetics term (Eq. 6).

Dimensionless Form of the Problem

Nondimensionalization of the set of equations

In this part, Eqs. 2 and 13 are written in a dimensionless form. For that, the dimensionless variables defined in Table 2 are used.

In Table 2, the absorbance ratio β_A describes the competition between the different species for absorbing the photons emitted at a given wavelength. If $\beta_A=1$, then compound A is the only absorbing species, and, if $\beta_A<1$, other species than reagent A (here the product B) absorb the photons at the wavelength considered. Thus, β_A will be called the competitive absorption factor.

Table 2. Dimensionless Variables

Dimensionless Variables	
$y^*=\frac{y}{W}$	$x^*=\frac{x}{L_c}$
$C_A^*=\frac{C_A}{C_{A0}}$	$C_B^*=\frac{C_B}{C_{A0}}=1-C_A^*$
$E_+^*=\frac{E^+}{\Lambda F_{wall}}$	$E_-^*=\frac{E^-}{\Lambda F_{wall}}$
$A_{e,A}^0=\kappa_A C_{A0} W$	$A_{e,B}^0=\kappa_B C_{A0} W$
$A_e^0=A_{e,A}^0+A_{e,B}^0=(\kappa_A+\kappa_B)C_{A0}W$	$\beta_A=\frac{A_{e,A}^0}{A_{e,B}^0}=\frac{\kappa_A}{\kappa_A+\kappa_B}$
$E^*=E_+^*+\upsilon E_-^*$	$\beta_B=\frac{A_{e,B}^0}{A_{e,B}^0}=\frac{\kappa_B}{\kappa_A+\kappa_B}=1-\beta_A$

The exponent "0" in the absorbances A_e^0, $A_{e,A}^0$, and $A_{e,B}^0$ means that the reference state chosen corresponds to the maximal absorbance that can be observed for each compound at the wavelength considered. The absorbance of the reactant A is maximal at the initial state (i.e., when $C_A=C_{A0}$), therefore $A_{e,A}^0=\kappa_A C_{A0} W$. The absorbance of the product B is maximal when the conversion of A is complete, namely, when $C_B=C_{A0}$, resulting in $A_{e,B}^0=\kappa_B C_{A0} W$. The definition of the total absorbance A_e^0 has been chosen so that the factor β_A is a constant that depends only on the molar absorption coefficients of the species (κ_A and κ_B). Indeed, if this absorbance is defined without reference, the factor β_A would depend on the concentrations C_A and C_B, and, thus, on the progress of the reaction. Consequently, A_e^0 does not refer to a real absorbance of the reaction medium: $A_e<A_e^0$. The reference state corresponds to the initial state only when a single compound absorbs incident photons ($\beta_A=1$). Finally, we can observe that A_e^0 is also the ratio of two characteristic lengths: the reactor width, W, and the optical thickness due to the absorbing species, $1/(\kappa_A+\kappa_B)C_{A0}$.

When introducing the dimensionless variables shown in Table 2, Eqs. 2 and 13 become

$$\begin{cases} \dfrac{6(1+\upsilon)}{A_e^0\Lambda Da_I}\left[(y^*)-(y^*)^2\right]\dfrac{\mathrm{d}C_A^*}{\mathrm{d}x^*}-\dfrac{(1+\upsilon)}{A_e^0\Lambda Da_{II}}\left(\dfrac{\mathrm{d}^2C_A^*}{\mathrm{d}y^{*2}}\right)= \\ \qquad -C_A^*\left(E_+^*+\upsilon E_-^*\right)=-C_A^*E^* \\ \dfrac{\mathrm{d}E_+^*}{\mathrm{d}y^*}=-A_e^0\Lambda\ \left[\beta_A C_A^*+\beta_B C_B^*\right]E_+^* \\ \dfrac{\mathrm{d}E_-^*}{\mathrm{d}y^*}=-A_e^0\Lambda\ \left[\beta_A C_A^*+\beta_B C_B^*\right]E_-^* \end{cases} \tag{16}$$

Characteristic times and physical significances of the governing dimensionless numbers

In Eq. 16, two dimensionless numbers commonly encountered in the reaction engineering field are highlighted: the Damköhler one and two numbers (Da_I and Da_{II}). Their definitions and expressions are given in Table 3.

As shown in Table 3, the Damköhler I and II numbers can be regarded as the ratio of the time characteristics of the phenomena encountered in a microreactor. For that, the characteristic time of the photochemical reaction $A\xrightarrow{h\nu}B$ should be consistently defined.

Characteristic Time of the Photochemical Reaction $A\xrightarrow{h\nu}B$. Typically, the characteristic time of a reaction is defined by

Table 3. Characteristic Times and Governing Dimensionless Numbers

Name	Symbol	Expression
Photochemical reaction time	τ_r	$\frac{WC_{A0}}{\Phi\beta_A F_{wall}(1+\upsilon)}$
Residence time	τ	$\frac{L_c}{\bar{u}}$
Transverse diffusion time	τ_d	$\frac{W^2}{D_m}$
Damköhler I	Da_I	$\frac{\tau}{\tau_r}=\Phi(1+\upsilon)\beta_A\left(\frac{F_{wall}}{C_{A0}W}\right)\left(\frac{L_c}{\bar{u}}\right)$
Fourier	Fo	$\frac{\tau}{\tau_d}=\frac{L_c}{\bar{u}}\frac{D_m}{W^2}$
Damköhler II	Da_{II}	$\frac{\tau_d}{\tau_r}=\frac{Da_I}{Fo}=\Phi(1+\upsilon)\beta_A\left(\frac{F_{wall}}{C_{A0}}\right)\frac{W}{D_m}$

$$\tau_r=\frac{C_{A0}}{r_A} \tag{17}$$

where r_A is the rate of consumption of the reactant A (expressed in mol m^3 s^{-1}).

For a photochemical reaction, as shown by Eq. 7, this rate is expressed by the product of the quantum yield Φ and the LVRPA (e_A^a). e_A^a is a function of the absorbance of the reaction medium (which depends on the progress of the reaction) and the geometry of both light source and photoreactor (which defines the irradiated surface, the fluid volume, and the photon fluence density at the reactor walls). Contrary to thermal reactions for which some intrinsic kinetic laws can be formulated (e.g., a first-order law), any generic expression of e_A^a, and, thus, of the rate r_A, can be established for a photochemical reaction as being specific to each light source/photoreactor system. This is all the more the case when, in many cases, numerical calculations are required to calculate e_A^a. This is undoubtedly one of the main difficulties encountered in photochemical reaction engineering, especially for scale-up purposes.

Under these assumptions made for describing the microphotoreactor's geometry and the incident light, we can demonstrate (see Supporting Information) that, for strongly absorbing media, the relevant definition of the characteristic time for a photochemical reaction $A\xrightarrow{h\nu}B$ is

$$\tau_r=\frac{C_{A0}W}{\Phi\beta_A F_{wall}(1+\upsilon)} \tag{18}$$

Note that the factor β_A which accounts for the competition between the species for absorbing incident photons appears in the expression of τ_r.

Physical Meaning of the Damköhler I Number. As reported in Table 3, Da_I is defined as the ratio between the residence time, τ, and the characteristic time of the photochemical reaction, τ_r. It can be regarded as a measure of the conversion that could be achieved: high values of Da_I will mean complete conversions at the outlet of the microreactor. It is interesting to note that Da_I is also directly linked to the dose, that is, to the amount of photons received during the residence time (einstein m^{-3}) per unit of reactor volume (einstein m^{-3}), defined as

$$Dose=\frac{q_p}{V_r}\tau=(1+\upsilon)\frac{F_{wall}}{W}\tau \tag{19}$$

where q_p is the photon flux received in the microreactor (einstein s^{-1}). The ratio $\frac{q_p}{V_r}$ depends on the photoreactor geometry, involving the irradiated surface areas and the microreactorvolume V_r: in the present case, it can be simply expressed as the ratio between F_{wall} and the reactor width/diameter W, weighted by $(1+\upsilon)$ to account for an illumination from one or both sides.

According to Eq. 19, the Damköhler I number, thus, can be expressed as

$$Da_I=\frac{\Phi}{C_{A0}}\beta_A Dose \tag{20}$$

The dose required to reach a given conversion depends logically on the competition factor β_A and on the medium absorbance A_e^0.

For weakly absorbing media, the exponential term in the photokinetic factor f is no longer negligible (see Supporting Information). In this case, the absorbance, averaged over a conversion varying between 0 and 1, is given by

$$\langle A_e^0\rangle=A_e^0\int_0^1[(1-X)\beta_A+X(1-\beta_A)]\mathrm{dX}=\frac{A_e^0}{2} \tag{21}$$

We can then demonstrate that the flux of photons absorbed per unit of reactor volume, averaged over a conversion varying between 0 and 1, should be weighed by the following factor to account for the medium transmittance

$$\left(1-e^{-\frac{A_e^0\Lambda}{2}}\right) \tag{22}$$

From this, a new characteristic time for the reaction, and, thus, a new Damköhler I number, can be defined, accounting for this averaged flux. Nevertheless, for clarity purposes, we chose not to define Da_I in sucha way.

Physical Meaning of the Damköhler II Number and of the Fourier Number. The Damköhler II number, Da_{II}, is defined as the ratio between the transverse mass transfer time (or transverse diffusion time), τ_d, and the characteristic time of the photochemical reaction, τ_r (Table 3). Therefore, it can be regarded as a measure of the efficiency of the mixing (namely of the mass transfer by molecular diffusion) along the optical light path (i.e., in the transverse direction y). The latter represents one of the two main phenomena responsible for the occurrence of concentration gradients in the transverse direction at the outlet of the microreactor. The occurrence of such concentration gradients can be induced:

- by the heterogeneous velocity field along the transverse direction. Due to the parabolic velocity profile in the microphotoreactor, the molecules close to the walls are transported by convection slower than the ones located at the center. The concentration gradients generated will annihilate if the transverse mass transfer time is smaller than the residence time, that is, if the Fourier number Fo is higher than one $Fo \geq 1$;
- and/or by the light attenuation along the optical light path. Due to this phenomenon, the reaction rate is heterogeneous in the transverse direction and will, thus, contribute to generate some concentration gradients. These gradients will induce a mass flux by molecular diffusion, which tends to oppose to the gradients generated. These two opposite phenomena are in competition, and the intensity of one with respect to the other is reflected by the Damköhler II number. Thus, a small value of Da_{II} means that the transverse diffusion characteristic time is shorter than the characteristic time of the photochemical reaction, and *a priori*, that the concentration will be homogeneous along the transverse direction at the outlet of the microreactor. For showing the importance

of such phenomena, we can imagine an extreme case in which the light is fully absorbed in a narrow zone close to the reactor wall (reacting zone). In that case, molecules of reagent A need to travel efficiently along the transverse direction y to reach the reacting zone where photons are available.

Naturally, these two phenomena are linked together because the following relation exists

$$Da_{II} = \frac{1}{Fo} Da_I \tag{23}$$

Equation 23 shows that, for a given Da_I, Da_{II} is linearly dependent on the inverse of the Fourier number $\frac{1}{Fo}$.

For a given set of these three dimensionless numbers (Da_I, Da_{II}, Fo), it is interesting to identify if some concentration gradients could exist along the transverse direction at the outlet of the microphotoreactor and, if so, what its origin is: the heterogeneous velocity field or the heterogeneous kinetic rate field (light attenuation). Figure 2 represents the variation of the Damköhler II number with the inverse of the Fourier number, for different Damköhler I numbers.

From Figure 2, four different zones can be identified, each being defined by a specific range of variation of (Da_{II}, Fo) numbers:

- Zone D corresponds to the case where Da_{II} and $\frac{1}{Fo}$ are inferior to one. In this zone, no concentration gradients are generated in the transverse section at the outlet of the microreactor in so far as the transverse diffusion time is smaller than the residence time and the reaction time. The concentrations can be, thus, considered homogeneous in the transverse direction at the outlet of the microreactor. This is the case where no diffusion limitations exist. This zone can be subdivided into two zones:
  - in the lower triangle where $Da_I < 1$, the conversion is not complete at the outlet of the microphotoreactor. Typically, a microphotoreactor will operate in this area when used as a tool for data acquisition: the residence time is varied to obtain different conversions at the outlet, for example, to establish a kinetic model;
  - in the upper triangle where $Da_I > 1$, the conversion is close to one at the outlet of the microreactor. As the concentration is transversally homogeneous at the outlet of the microreactor, one can use a plug-flow model: this is the operating regime that is looked for when the microphotoreactor is used for production.
- Zone A corresponds to $Da_{II} \geq 1$ and $(1/Fo) \leq 1$. The concentration gradients generated are here only due to the heterogeneous kinetic rate field ($\tau_r < \tau_d$ and $\tau_d < \tau$). Generally, as shown in Figure 2, when the microreactor operates in this zone, the conversion is complete before the outlet: this is a nonideal use of the microphotoreactor, as implying that the product of the reaction is over-exposed to the radiations, which can induce subsequent photo-decomposition.
- Zone C corresponds to $Da_{II} \leq 1$ and $(1/Fo) \geq 1$. Some concentration gradients are here generated due to the heterogeneous velocity field ($\tau_r > \tau_d$ and $\tau_d > \tau$). In this zone, the Damköhler I numbers are low, and so are the conversions at the outlet. When the microphotoreactor is used as a tool for data acquisition, it is essential to ensure that it does not operate in this zone and isused to determine not intrinsic kinetic data, but apparent ones.
- Zone B corresponds to $Da_{II} \geq 1$ and $(1/Fo) \geq 1$. The concentration gradients generated are here due to both the heterogeneous velocity and the heterogeneous kinetic rate fields. The microphotoreactor deviates from a plug-flow behavior. The operating regime of the microphotoreactor is, thus, not ideal, as the conversion (or the selectivity) will be affected by the occurrence of these concentration gradients.

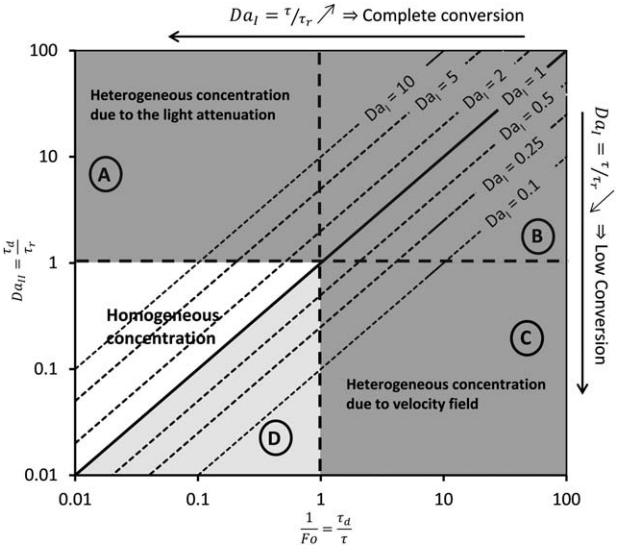

Figure 2. Diagram linking the governing dimensionless numbers Da_I, Da_{II}, and Fo.

At last, it is relevant to note that the small dimensions of microphotoreactors induce a decrease of the values of Da_{II} and of $1/Fo$, and thus, make in general the microreactors operating in Zone D. Nevertheless, this is not systematic (in particular as it is depending on the photon flux received, which controls the time characteristic of the photochemical reaction), and so, Figure 2 can be a practical tool to check in which zone (A, B, C, or D) a given microphotoreactor operates.

Solving of the problem and output variables

The set of equations involved in Eq. 16 is numerically solved by a finite element method with the help of the Comsol® (version 4.3b) software. A structured mesh with triangular regular elements was used. The sensibility of the number of elements in the mesh was investigated and an optimal number of elements ($40\ 10^3$) was determined in order not to influence the solution and to maintain reasonable calculations times. In each calculation, the mass balance between reactor inlet and reactor outlet was checked. The validity of the numerical method implemented was checked using two limit cases (see Supporting Information).

All the results will be presented in terms of dimensionless numbers. For illustration, some typical values encountered in microphotoreactors are given here: L_c varying from 0.1 to 1 m, W varying from 100 to 1000 μm, F_{wall} varying from 10^{-3} to 10^{-5} einstein m^{-2} s^{-1}, Φ varying from 0.1 to 1 (quasi-stoichiometric reaction), C_{A0} varying from 0.1 to 1000 mol m^{-3}.

The model implemented (Eq. 16) gives access to the local values of the concentration of each species, $C_i(x,y)$, and to the local volumetric rate of photon absorbed by each species, $e_i^a(x,y)$. From these local values, various averaged quantities are computed to analyze the results.

The conversion at the outlet of the microreactor is determined as the ratio between the average molar fluxes of the reagent A at the outlet ($x^*=1$) and at the inlet ($x^*=0$)

$$X=1-\frac{\int_{S_{\text{outlet}}} u\ C_A \mathrm{d}S}{\int_{S_{\text{inlet}}} u\ C_A \mathrm{d}S}=1-\frac{\left(\int_0^1 u\ C_A \mathrm{d}y^*\right)^{x^*=1}}{\left(\int_0^1 u\ C_A \mathrm{d}y^*\right)^{x^*=0}} \tag{24}$$

The average volumetric rate of photons absorbed by the species i, $<e_i^a>$ is obtained by averaging the local values in the entire domain (reactor volume)

$$<e_i^a> \ = \frac{1}{V_r}\int_{V_r} e_i^a \mathrm{d}V=\frac{1}{L_c W}\int_{x^*=0}^{x^*=1}\int_{y^*=0}^{y^*=1} e_i^a \mathrm{d}y^* \mathrm{d}x^* \tag{25}$$

where V_r is the reactor volume (i.e., the $V_r=L_c * W$ as a 2-D geometry is assumed)

From $<e_i^a>$, it is interesting to introduce the coefficient Γ defined as

$$\Gamma=\frac{<e_A^a>}{<e_A^a>+<e_B^a>} \tag{26}$$

This coefficient Γ enables to evaluate the amount of photons absorbed by the compound A per unit of time and per unit of volume with respect to the total amount of photons absorbed per unit of time and per unit of volume. For the chosen photochemical reaction $A\xrightarrow{h\nu}B$, $(1-\Gamma)$ represents the part of the photons absorbed by the product B.

The photonic efficiency at a given conversion X, defined, according to Aillet et al. ([23]),[23] from the irradiance time, t_X, (assumed equal to the residence time) and from the number of moles of the compound A converted, n_r, can be also calculated

$$\eta^X \ =\frac{n_r}{\phi q_p t_X}=\frac{C_{A0}\ X}{\phi}\frac{W}{(1+\upsilon)F_{wall}}\frac{1}{\tau}=\frac{C_{A0}\ X}{\phi}\frac{1}{Dose} \tag{27}$$

Subsequently, the productivity at a given conversion X is given by

$$R^X \ =\frac{n_r}{t_X}=\phi q_p \eta^X=\phi S_{\text{exposed}}(1+\upsilon)F_{wall}\eta^X=\ \frac{C_{A0}\ X}{Dose} \tag{28}$$

Where S_{exposed} is the surface of the reactor exposed to the radiations.

Results on the Effect of Diffusion Limitations

In this section, the conversion at the exit of the microphotoreactor and the photonic efficiency will be investigated as a function of the dimensionless numbers previously defined

$$\begin{cases} X=X(Da_I, Da_{II}, A_e^0, \beta_A,) \\ \eta^X=\eta^X(Da_I, Da_{II}, A_e^0, \beta_A) \end{cases} \tag{29}$$

The case where the microphotoreactor can be described as a PFR ($Da_{II}\rightarrow 0$) will be considered first. The influence of diffusion limitations along the optical light path (i.e., along the microreactor width) will be subsequently studied.

No diffusion limitations (PFR, $Da_{II}\rightarrow 0$)

Impact on the Conversion. If $Da_{II}\rightarrow 0$, the diffusion term in Eq. 2 tends toward zero and the velocity field is reduced to a constant mean velocity $\bar{u}$. In this particular case, the equations related to the spherical irradiances E^+ and E^- can be integrated separately (as done in Supporting Information) and directly introduced in the transport equation, as

$$\frac{6\left[(y^*)-(y^*)^2\right]}{A_e^0\beta_A Da_I}\frac{\mathrm{d}C_A^*}{\mathrm{d}x^*}= -\Lambda C_A^*\left(e^{-A_e^0\Lambda\ \left[\beta_A C_A^*+\beta_B C_B^*\right]y^*}+\upsilon e^{-A_e^0\Lambda\ \left[\beta_A C_A^*+\beta_B C_B^*\right](1-y^*)}\right) \tag{30}$$

By averaging Eq. 30 along the transverse direction ($0\le y^*\le 1$), and by introducing the conversion, the following equation is obtained

$$\begin{cases} \frac{\mathrm{d}X}{\mathrm{d}x^*}=Da_I f \\ f=\frac{(1-X)}{[\beta_A(1-X)+(1-\beta_A)X]}\left(1-\exp\left(-A_e^0\Lambda[\beta_A(1-X)+(1-\beta_A)X]\right)\right) \end{cases} \tag{31}$$

Equation 31 is a nonlinear ordinary differential equation. The conversion X can be, thus, be calculated by numerical integration of Eq. 31 from $(x^*=0\ ;\ X=0)$ to $(x^*=1\ ;\ X)$. This has been performed for different sets of the values of Da_I, β_A, and A_e^0, thus enabling a large database, $X=f(Da_I, \beta_A, A_e^0)$, to be created.

In Figure 3A, the Damköhler I number Da_I required to reach a conversion of 95% is plotted as a function of the absorbance A_e^0, for different competitive absorption factors β_A. Note that the value of 95% has been chosen as an illustrative case of quasi-complete conversion. Alternative choices would not differ from the results obtained. For $A_e^0\ge 5$ (strong absorbing media), Da_I tends toward an asymptotic value, specific to each value of β_A: Da_I thus becomes independent from the absorbance of the absorbing media. Da_I being linked to the dose (Eq. 20), the dose required does not depend on the absorbance anymore when the latter is important. In addition, Figure 3A shows that the Damköhler I number required to reach a conversion of 95% increases when the competitive absorption factor β_A decreases. For example, for $\beta_A=1$, $Da_I\approx 1$ whereas for $\beta_A=0.1$, $Da_I\approx 2$. This means that the dose required should be multiplied by a factor 20 between a medium where $\beta_A=1$ and a medium where $\beta_A=0.1$.

For low absorbing media ($A_e^0\le 5$), the values of Da_I required increase significantly when the absorbance A_e^0 decreases: for example, if $\beta_A=1$, for $A_e^0=1$, $Da_I\approx 3.5$, and for $A_e^0=3$, $Da_I\approx 1.6$. This can be explained by the fact that the time characteristic of the photochemical reaction, τ_r, is defined for strongly absorbing media (Eq. 18, see also Supporting Information), and thus that the exponential factor $\left(1-e^{-\frac{A_e^0\Lambda}{2}}\right)$ accounting for the medium transmittance is neglected in the definition of τ_r. In Figure 3B, the variation of the Damköhler I number corrected by the factor $\left(1-e^{-\frac{A_e^0\Lambda}{2}}\right)$ is represented as a function of the absorbance A_e^0. In this form, the values of Da_I required to reach a conversion of 95% are now much closer to each other, and therefore, independent from the absorbance A_e^0.

All these findings confirm the importance of the definition chosen for τ_r. Whatever the absorbance A_e^0 and the competitive absorption factor β_A, a quasi-complete conversion (95%) is reached at the outlet of the microreactor when

$$1\le\left(1-e^{-\frac{A_e^0\Lambda}{2}}\right)Da_I\le 2 \tag{32}$$

This is in agreement with the interpretation of Da_I for thermal reactions for which a value slightly higher than one

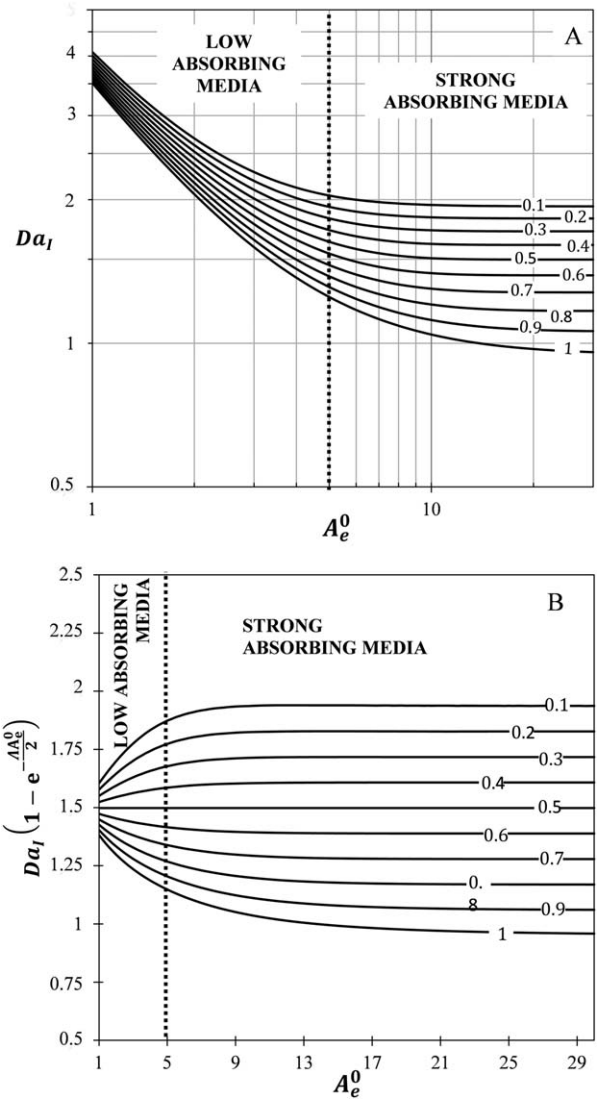

Figure 3. Variation of the Damköhler I number (A) and of the Damköhler I number corrected by the exponential factor (Eq. 22) (B) required to reach a conversion of 95% with the absorbance A_e^0 Each curve is associated with a competitive absorption factor β_A.

represents a complete conversion at the outlet of the microreactor.

It is interesting to study the case of strongly absorbing media. Indeed, for high values of A_e^0, the exponential term of Eq. 31 can be neglected, leading to the following equation

$$\left(\frac{\beta_A(1-X)+(1-\beta_A)X}{1-X}\right)\mathrm{d}X=Da_I\mathrm{d}x^* \tag{33}$$

By integrating Eq. 33 from $x^*=0$ to $x^*=1$, the following relationship is obtained

$$-(1-\beta_A)(X+\ln(1-X))+\beta_A X=Da_I=\beta_A\frac{\Phi}{C_{A0}}\mathrm{Dose} \tag{34}$$

From Eq. 34, it becomes apparent again that for strong absorbing media, the Damköhler I number does not depend anymore on the absorbance A_e^0. This relationship is particularly suitable for rapid engineering calculations: it then enables an easy determination of the dose (i.e., the amount of photons received per unit of reactor volume, in einstein m^{-3}) required to reach a given conversion (here 95%), which is the key parameter for designing a continuous microphotoreactor. One should keep in mind that Eq. 34 is valid only for $A_e^0 \geq 5$ (See Supporting Information).

A parallel can be drawn between the dose in a microphotoreactor and the residence time in a microreactor operating with a thermal reaction. In the latter case, the residence time is adjusted by changing the flow rate or the reactor volume, whereas, in microphotoreactors, the dose (Eq. 19) additionally depends on the photon fluence density at the reactor walls F_{wall}, thus giving an additional degree of freedom.

As an illustration, two microphotoreactors, 1 and 2, with two different widths $(W)_1$ and $(W)_2$, as defined in Table 4, are exemplarily compared. In the two microphotoreactors, the absorbance A_e^0 is assumed higher than five so as it is possible to apply Eq. 32 (for that, the initial concentration of the compound A has to be adjusted). Suppose also that some preliminary runs have been performed in the microphotoreactor 1 to find the suitable dose required to reach a given conversion X at the outlet of the microreactor. Depending on the photon flux density at the reactor walls F_{wall}, the residence time required is calculated, according to Eq. 19, as: $(\tau)_1=\left(\mathrm{Dose}\frac{W}{F_{wall}}\right)_1$. The photochemical reaction is then transferred to a larger scale in microphotoreactor 2. As already discussed, to obtain the same conversion, the dose has to be maintained, meaning that $(Dose)_1=(Dose)_2$. For that, either the residence time $(\tau)_2$ or the photon flux density at the reactor walls $(F_{wall})_2$ must be four times higher in this microphotoreactor $(\tau F_{wall})_2=4\times(\tau F_{wall})_1$.

A final specific scenario can be considered, the one where the conversion at the outlet of the microreactor is low. In this case, the amount of the product B formed is so that it will not significantly absorb the incident photons. We can, thus, consider a single absorbing species, namely $\beta_A=1$. Equation 31 then has an analytical solution

$$Da_I=\left(X+\frac{1}{A_e^0}\ln\left[\frac{1-\exp(-\Lambda A_e^0)}{1-\exp(-\Lambda A_e^0(1-X))}\right]\right) \tag{35}$$

Note that, even if expressed in a dimensionless form, Eq. 35 is similar to the one established by Aillet et al.[23] in the case of an intramolecular [2+2] photocycloaddition, where only the reactant (i.e., the Diels-Alder compound) absorbed the incident photons.

Impact on the Photonic Efficiency. The photonic efficiency defined in Eq. 27 is an interesting parameter which allows to evaluate the optimal use of photons. Indeed, it is defined as the ratio between the number of mole of compound B produced and the number of mole of photons received in the microphotoreactor. Based on the photochemistry principles, not all of the photons absorbed necessarily lead to the conversion of the compound A. This is quantified by the quantum yield of the reaction. However, other

Table 4. Comparison of Two Microphotoreactors

Microphotoreactor 1	Microphotoreactor 2
$(W)_1$	$(W)_2=4*(W)_1$
$(F_{wall})_1$	$(F_{wall})_2$
$(A_e^0)_1$	$(A_e^0)_2$
$(C_{A0})_1$	$(C_{A0})_2$
β_A	β_A

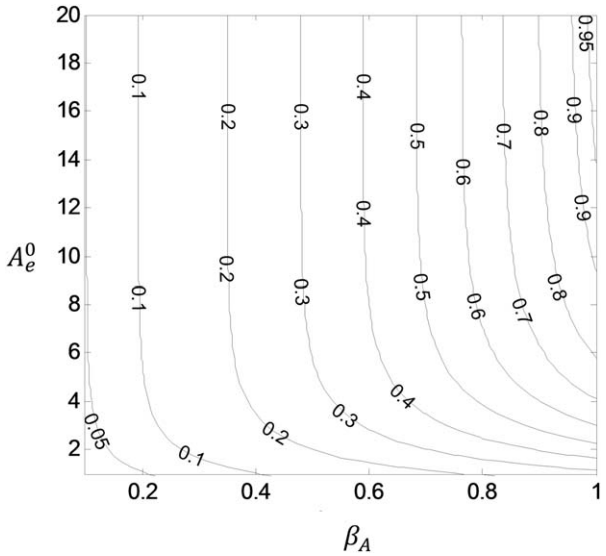

Figure 4. Iso-curves for photonic efficiency (for a conversion of 95%) as a function of the dimensionless numbers A_e^0 and β_A.

phenomena can increase the number of photons required to form the product B:

- the hydrodynamics inside the reactor: when the product B or other molecules absorb the incident photons, poor mixing conditions can generate an overexposure of these molecules to the detriment of the reactant A, and thus reduce the part of photons available for A;
- the transmittance of the material: if the medium absorbance is low, a significant part of the photons are transmitted over the back side wall of the reactor if the latter is transparent (no reflector). In this case, it is necessary to irradiate over longer periods to offset the loss of photons by transmittance.

The photonic efficiency η^X enables the two latter phenomena (mixing and transmittance) to be taken into account. Note that it has been corrected by the quantum yield to free it from the effects of deactivation processes intrinsic to the photochemical reaction mechanisms. Ideally, the photonic efficiency η^X is 1, thus meaning that one mole of photons was used to form one mole of product.

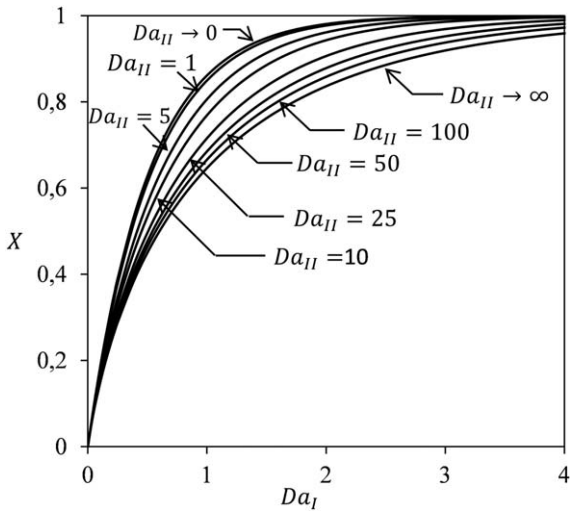

Figure 5. Conversion at the exit of the microreactor vs. Da_I for different Da_{II} (A_e^0=10, β_A=0.5, Λ=υ=1).

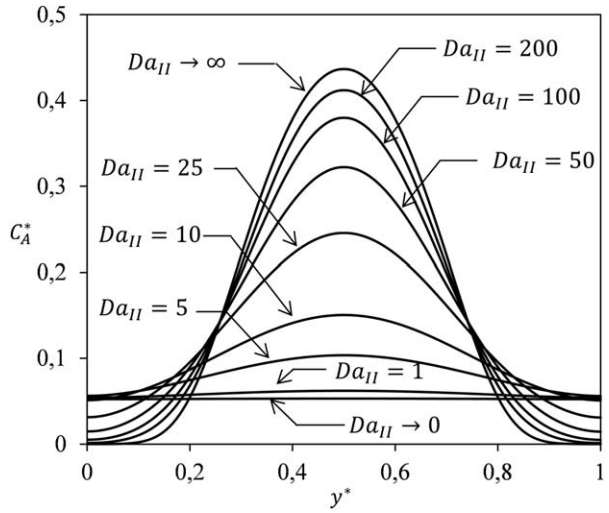

Figure 6. Transverse profiles of dimensionless concentration profiles of compound A at the reactor outlet for different Da_{II} (Da_I=1.5, A_e^0=10, β_A=0.5, Λ=υ=1).

From Eqs. 19 and 27, the photonic efficiency can be also expressed as

$$\eta^X = \frac{\beta_A X}{Da_I} \tag{36}$$

Thus, based on database $X=f(Da_I, \beta_A, A_e^0)$ elaborated in the previous section, a new database $\eta^X=f(A_e^0, \beta_A, X)$ is established. From this, Figure 4 can be constructed, giving the iso-curves of photonic efficiency (for a conversion X of 95%) as a function of the absorbance A_e^0 and the competitive absorption factors β_A. Two main comments can be made:

- for a given β_A, the more the media is absorbing (high A_e^0), the more the photonic efficiency tends to its optimal value (η^X=1). All the photons are then absorbed in the medium, or in other words, no photons are lost by transmission over the back wall of the microreactor;
- for low β_A, the photonic efficiency decreases strongly, even for high absorbances A_e. This is due to the fact that the main portion of photons is absorbed by the product $B_{h\nu}$.

When operating the photochemical reaction $A \xrightarrow{h\nu} B$ in microreactors, the decrease in the photonic efficiency due to β_A cannot be overcome, as β_A (defined from the ratio of molar absorption coefficients) is an intrinsic property of the reaction. Nevertheless, the decrease in the photonic efficiency due to the absorbance A_e^0 can be overcome by increasing the concentration of the compound C_{A0} (in the limit of the solubility) or the reactor width (W); that is, of course, desirable from an economical point of view since it means that less photons need to be provided for the reaction.

Influence of diffusion limitations ($Da_{II} \neq 0$)

This section aims at investigating how mass transfer by diffusion along the microphotoreactor's width can affect the conversion at the exit. For pedagogic purposes, the following operating conditions are retained:

- the absorbance A_e^0 is put equal to 10, meaning that light is entirely absorbed in the medium (no transmission over the back wall of the microreactor);

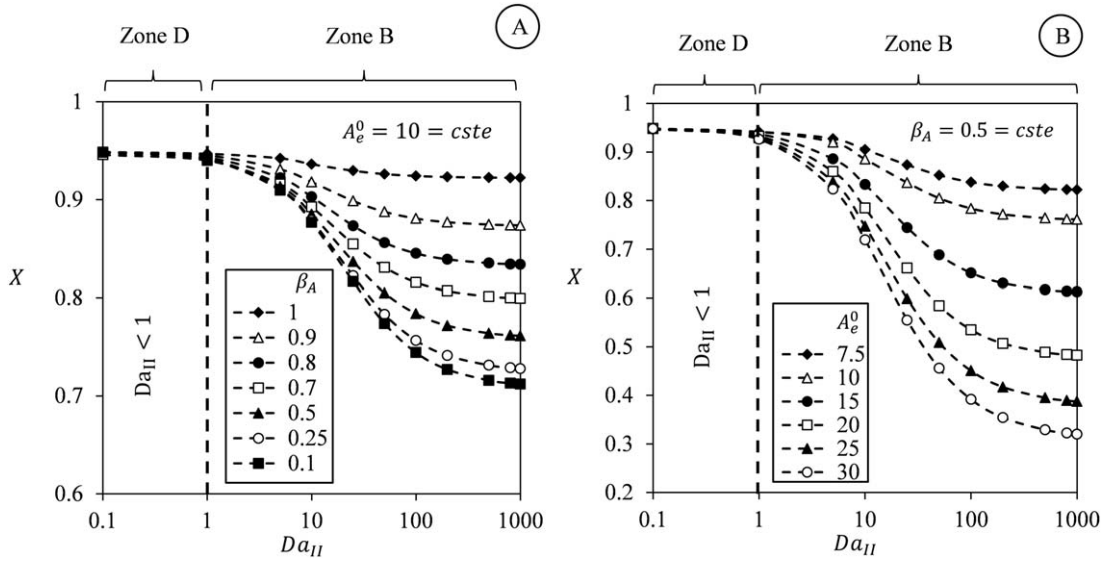

Figure 7. Variation of the conversion at the exit of the microreactor as a function of Da_{II}: (A) for different β_A and a fixed absorbance (A_e^0=10), (B) for different A_e^0 and a given competitive absorbance factor (β_A=0.5).

• compounds A and B are supposed to equivalently absorb incident photons, that is, β_A=0.5 (in this particular case, the absorbance does no longer depend on the conversion);

• the radiation field is supposed collimated (i.e., Λ=1) and the microreactor is illuminated from both sides (i.e., υ=1).

Impact on the Conversion. Figure 5 presents the variation of the conversion X at the reactor's exit as a function of Da_I for different Da_{II} varying between two limits cases: $Da_{II} \to \infty$ and $Da_{II} \to 0$. It clearly appears that, for a given Da_I, the conversion decreases when increasing Da_{II}. For example, for Da_I=1, the conversion is almost equal to 0.9 when $Da_{II} \to 0$, whereas it drops to 0.65 when $Da_{II} \to \infty$. This demonstrates that the mass transfer by diffusion along the transverse direction can be a factor that significantly limits the conversion, even in microphotoreactors.

In Figure 6, the transverse profiles of the dimensionless concentration of the compound A at the outlet of the microphotoreactor, $C_A^*(y^*)$, are shown for Da_I=1.5 and different Da_{II}. We can observe that, for $Da_{II} \geq 1$, the profiles are no more homogeneous. As expected, strong concentration gradients at the outlet of the microphotoreactor appear as far as Da_{II} increases, that is, when the transverse diffusion phenomenon becomes slower and slower. It corresponds to zone B (Figure 2), where both the characteristic time of the photochemical reaction and the residence time are shorter than the transverse diffusion time.

In Figure 7, the conversion at the exit of the microreactor is plotted as a function of the Damköhler II number, for values of Da_I which correspond to a conversion of 95% in the case of a PFR (i.e., when $Da_{II} \to 0$). In Figure 7A, the absorbance A_e^0 is fixed at 10 (entirely absorbing medium) and different levels of competitive absorption (β_A) are presented. For $\beta_A < 1$, a significant decrease in conversion is observed when increasing Da_{II}: for example, for Da_{II}=1000, X=0.7 when β_A=0.1 and X=0.87 when β_A=0.9. In Figure 7B, the variation of the conversion with Da_{II} is also represented, but this time for a competitive absorption factor β_A fixed at 0.5 and different absorbance values A_e^0. The same tendencies for the conversion are obtained. However, for high Da_{II}, the conversion is strongly impacted by the degree of the medium absorbance. For example, when $Da_{II} \to \infty$, X =0.32 for A_e^0=30 whereas X=0.78 for A_e^0=10. At last, both Figures 7A,B show that all the curves (associated with different absorbance or with competitive absorption factors) are regrouped around an unique curve when $Da_{II} < 1$, and separate each other when $Da_{II} > 1$. This result confirms the importance of the time characteristic for the photochemical reaction as defined in Eq. 18.

The heterogeneous concentration field inside the reactor (illustrated in Figure 6) is responsible for the decrease of the conversion at the reactor exit observed in Figures 5 and 7. To understand this, it is interesting to compare the average local volumetric rates of photons absorbed by the compounds A and B inside the reactor ($<e_A^a>$ and $<e_B^a>$ expressed in einstein m^{-3} s^{-1}). For that, the ratio Γ defined in Eq. 26 is reported in Table 5. Whatever the values of Da_{II}, the total amount of photon absorbed is constant but the contribution of the amount of photons absorbed by each species changes depending on Da_{II}. In particular, the amount of photons absorbed by the compound A decreases as Da_{II} increases (i.e.,Γ decreases), thus explaining the lower conversions obtained at the reactor outlet. This latter phenomenon is

Table 5. Repartition of the Average Volumetric Rate of Photon Absorption for Different Da_{II}

Da_{II}	$<e_A^a>$ (einstein m^{-3} s^{-1})	$<e_B^a>$	$<e_A^a> + <e_B^a>$	$\Gamma = \frac{<e_A^a>}{<e_A^a>+<e_B^a>}$
0	318	675	993	0.321
1	316	677	993	0.318
5	306	687	993	0.309
10	297	696	993	0.299
25	281	712	993	0.283
50	270	723	993	0.272
100	263	730	993	0.265
200	259	734	993	0.261
500	256	737	933	0.258
800	255	738	993	0.257
∞	255	738	933	0.257

These values are computed for a conversion of 95% (Da_I=1.5,A_e^0=10, β_A=0.5, Λ=1, υ=1).

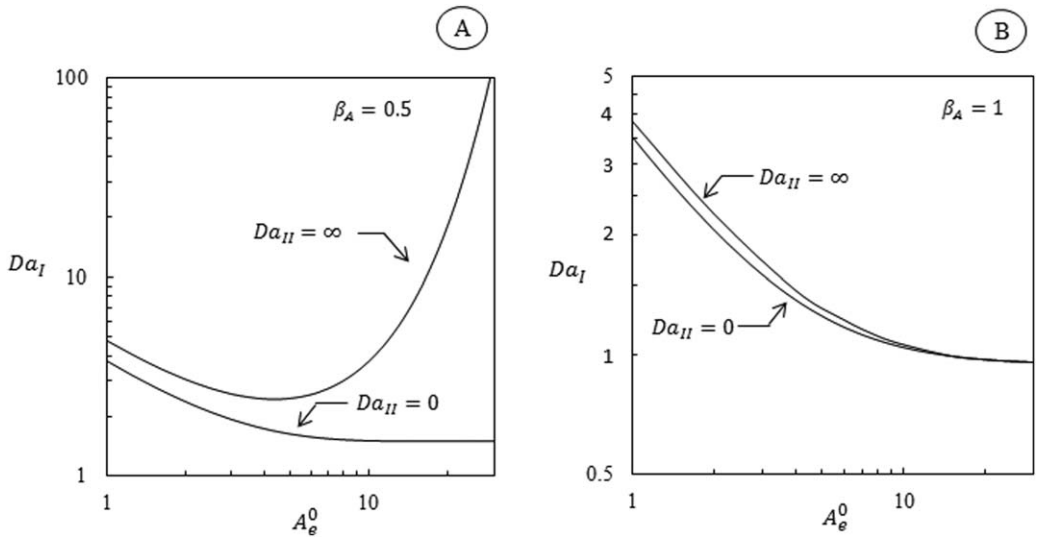

Figure 8. Variation of Da_I required to reach a conversion of 95% with the absorbance for the two limits cases ($Da_{II}=0$ and $Da_{II}=\infty$). (A) $\beta_A=0.5$, (B) $\beta_A=1$. The microreactor is illuminated from both sides ($\upsilon=1$) and $\Lambda=1$.

directly due to the formation, from the initial moments of the reaction, of a film of compound B close to the reactor wall where the light is the most intense. As the compound B absorbs at the same wavelength than the compound A ($\beta_A < 1$), this film (or layer) of compound B generated at the walls plays the role of a screen or a filter, which prevents the photons to penetrate inside the reactor and to react with the compound A. This film persists throughout the microreactor length as the mass transfer by diffusion does not enable the fluid at the reactor wall to be efficiently renewed. Note that the occurrence of such film/layer can be also visualized when representing concentration and volumetric rates of photon absorption fields in the microphotoreactor (see Supporting Information).

As aforementioned, the stronger the absorbance of the medium, the more pronounced the effect of Da_{II} is. To highlight that, the variation of the Damköhler I number required to reach a conversion of 95% with the absorbance is presented for two limit cases ($Da_{II} \to 0$ and $Da_{II} \to \infty$), for $\beta_A=0.5$ in Figure 8A and for $\beta_A=1$ in Figure 8B. For high absorbances A_e^0, we can observe that:

- when no diffusion limitation exists ($Da_{II} \to 0$), Da_I tends toward an asymptotic value as already observed in Figure 3A;
- in the presence of diffusion limitations ($Da_{II} \to \infty$), for $\beta_A=0.5$, the values of Da_I (and thus the dose) increase exponentially with A_e^0. The absorbing layer is not renewed, a significant part of the molecules of A remains nonirradiated, and thus, the dose required to reach a conversion of 95% should be increased.

For low absorbances A_e^0 and for $\beta_A=0.5$, the values of Da_I required to reach a conversion of 95% are very close whether the transverse diffusion phenomenon is slow or not. This is directly due to the transparency of the medium and the absorbing layer covers all the microreactor depth. Molecules no longer need to migrate into the absorbing layer as they are already in it.

When A is the single absorbing species (Figure 8B), the efficiency of the transverse diffusion slightly impacts on the values of Da_I, and thus the dose required: for $1 \le A_e^0 \le 30$, the difference is smaller than 10%. This can be explained by the fact that the absorbing layer shifts to the center of the microreactor as far as the conversion progresses. This is a key finding for microreactor modeling.

In summary, the main concluding remarks can be drawn:

- if there is no photon absorption competition inside the reactor (i.e., $\beta_A=1$), the conversion at the exit of the microreactor can be modeled by considering a PFR behavior;
- if the reagent A and the product B absorb photons at the same wavelength ($\beta_A < 1$), depending on the absorbance, the conversion for a given dose received in the microreactor is affected by the transverse diffusion. This phenomenon is observed because a layer of compound B accumulates close to the reactor wall.

Impact on the Photonic Efficiency. As shown in Eq. 36, the photonic efficiency η^X is linked to the Damköhler I

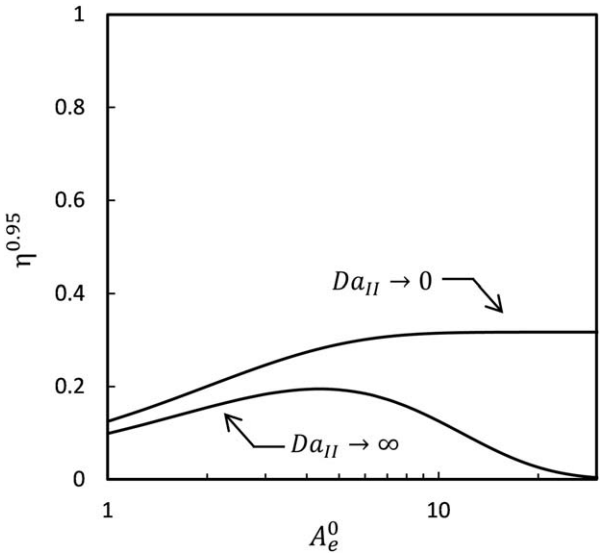

Figure 9. Evolution of the photonic efficiency with the absorbance for the two limits cases $Da_{II} \to 0$ and $Da_{II} \to \infty$ ($\beta_A=0.5$, $\upsilon=1$, $\Lambda=1$).

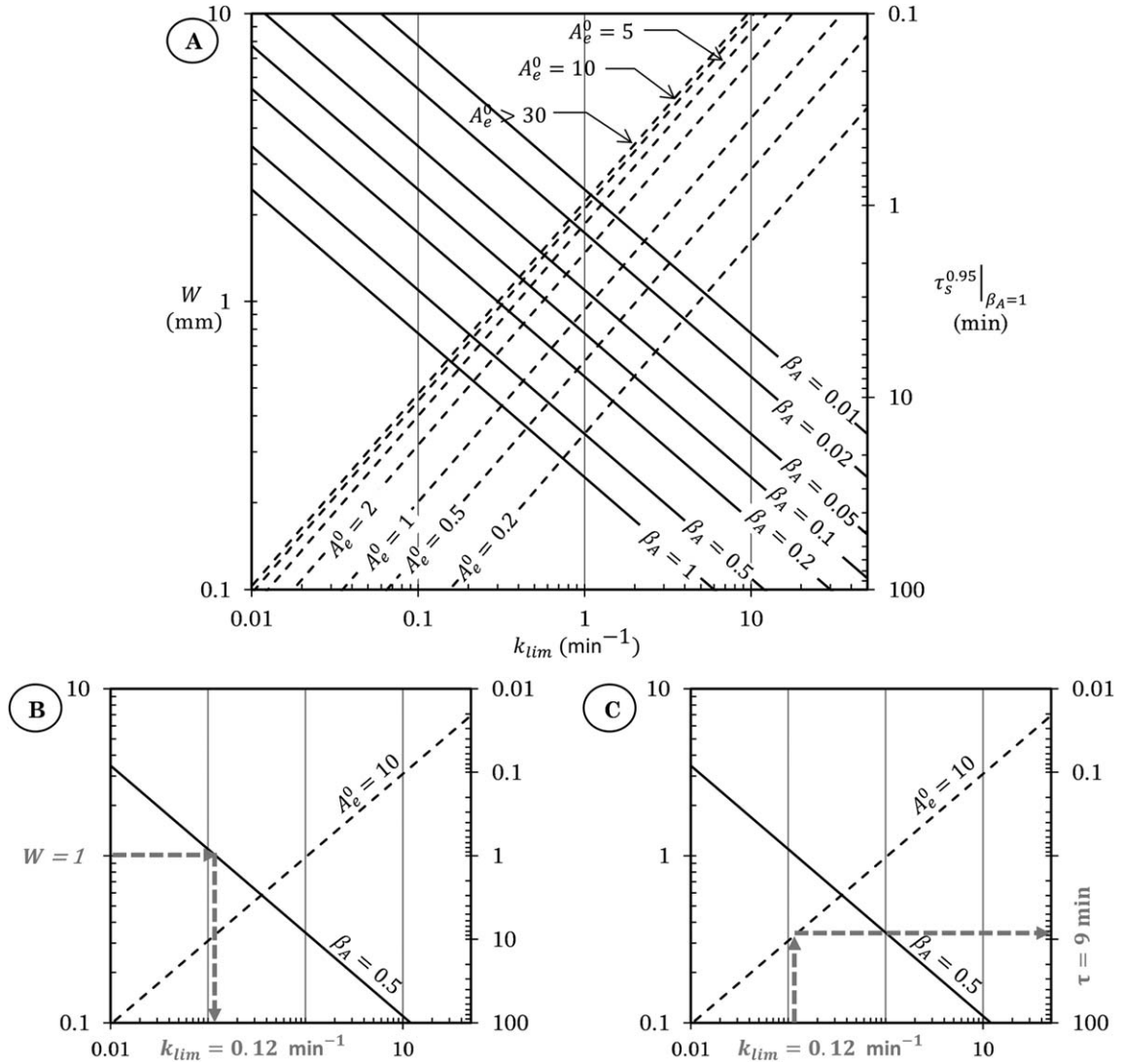

Figure 10. Diagram representing the microreactor width and the residence time required to reach a conversion of 95% in the case where β_A=1 as a function of the coefficient *k* for different absorbances and competitive absorption factors. (A): complete view, (B) and (C): zoomed views.

number, and thus to the dose of photons. The results presented in the latter section have clearly demonstrated how the mass transfer by diffusion along the microreactor depth can strongly influence the Da_I required to reach a given conversion. Logically, this phenomenon will also impact on the photonic efficiency.

In Figure 9, the photonic efficiency (for a conversion X of 95%) is plotted as a function of A_e^0 for the two cases: $Da_{II} \rightarrow 0$ and $Da_{II} \rightarrow \infty$ (the conditions are the same than in Figure 8). When the microreactor tends toward a PFR ($Da_{II} \rightarrow 0$), the photonic efficiency is improved when increasing values of A_e^0 until reaching an asymptotic value. On the contrary, when the microreactor deviates strongly from a PFR ($Da_{II} \rightarrow \infty$), the photonic efficiency falls to zero for the highest values of A_e^0. Therefore, the occurrence of transverse diffusion limitations has three main consequences:

- the amount of photons emitted by the lamp should be increased to be able to reach the desired conversion, which is not energetically efficient since more photons are required for the reaction;
- the amount of photons absorbed by the compound B increases significantly when rising Da_{II}. Special attention should be paid to this fact that, in the case of light-sensitive products, some photodecomposition may occur and may, thus, impact on the reaction selectivity;
- if the microreactor operates in such limiting conditions (zone B in Figure 2), it is advisable to work with low absorbance for optimizing η^X.

Some Guidelines to Avoid Diffusion Limitations

Microphotoreactor operation to avoid transverse diffusion limitations (i.e., to maintain Da_{II}=1)

As demonstrated in the previous sections, Da_{II} plays a crucial role and significantly affects the conversion at the microreactor exit and the photonic efficiency. For this reason, and also for upscaling purposes, it is interesting to understand how Da_{II} can be modified in practice (i.e., in terms of operating parameters). For a given set of operating conditions (A_e, β_A, $C_{A,0}$, W), Table 3 shows that Da_{II} is easily lowered by decreasing the photon flux

density at the reactor wall (F_{wall}). Therefore, to keep $Da_{II} \leq 1$ (i.e., to operate in zone D in Figure 2), the maximum photon flux density at the reactor wall can be calculated for a given microreactor width W and a given set of reactional medium properties (C_{A0}, β_A, Φ). The accurate knowledge of the diffusion coefficient D_m being not trivial, a value of 10^{-9} m^2 s^{-1} will be assumed as a first approximation.

When no diffusion limitation exists ($Da_{II} \underset{\rightarrow}{} 0$), it has been shown that the problem can be formulated by considering a PFR behavior, according to Eq. 31. Based on the idea presented by Nagy et al.,[44] Eq. 31 can also be written, when considering the definition of Da_I (Table 3) and considering d $\tau = \tau dx^*$ as

$$\begin{cases} (1+\upsilon)\beta_A \dfrac{\Phi}{C_{A0}} \dfrac{F_{\text{wall}}}{W} d\tau = \dfrac{dX}{f} \\ f = \dfrac{(1-X)}{[\beta_A(1-X)+(1-\beta_A)X]} \left(1-\exp\left(-A_e^0 \Lambda[\beta_A(1-X)+(1-\beta_A)X]\right)\right) \end{cases} \tag{37}$$

The integration of Eq. 37 leads to

$$\frac{Da_I}{\beta_A} = k\tau^X = \chi^X \tag{38}$$

With

$$\begin{cases} k = (1+\upsilon)\dfrac{\Phi}{C_{A0}} \dfrac{F_{\text{wall}}}{W} = \dfrac{\chi^X}{\tau^X} \\ \chi^X = \dfrac{1}{\beta_A} \displaystyle\int_0^X \frac{1}{f} dX \end{cases} \tag{39}$$

And τ^X is the residence time required to reach a conversion X.

Note that k is dimensionally equivalent to the inverse of time and, thus, can be compared to a kinetic rate constant of a thermal one order reaction.

Thus, using the expression of k, Da_{II} can be expressed as

$$Da_{II} = \Phi(1+\upsilon)\beta_A \frac{F_{wall}}{C_{A0}} \frac{W}{D_m} = \beta_A k \frac{W^2}{D_m} \tag{40}$$

For a given microreactor width, W, and a given competitive absorption β_A, the coefficient k such as $Da_{II} = 1$ can be calculated from Eq. 40, as

$$k = \frac{1}{\beta_A} \frac{D_m}{W^2} \tag{41}$$

Based on Eq. 40, Figure 10 in which the microreactor width, W, is plotted as a function of the coefficient k for different competitive absorption factor β_A, can be built. It has been deliberately chosen, with regard to the characteristic dimension encountered in microreactors, to express the microreactor W in mm and k in min^{-1}.

Then, the residence time required to reach a conversion, X, of 95%, $\tau^{0.95}$, can be estimated at a given absorbance A_e^0 and at a given competitive absorption factor β_A. For that, $\chi^{0.95}$, which depends on A_e^0 and on β_A (Eqs. 37 and 39), should be first calculated by numerical integration. Following this approach, $\tau^{0.95}$ is deduced from the ratio between $\chi^{0.95}$ and k (Eq. 39).

Function H is introduced, defined for a given conversion (here 95%), such as

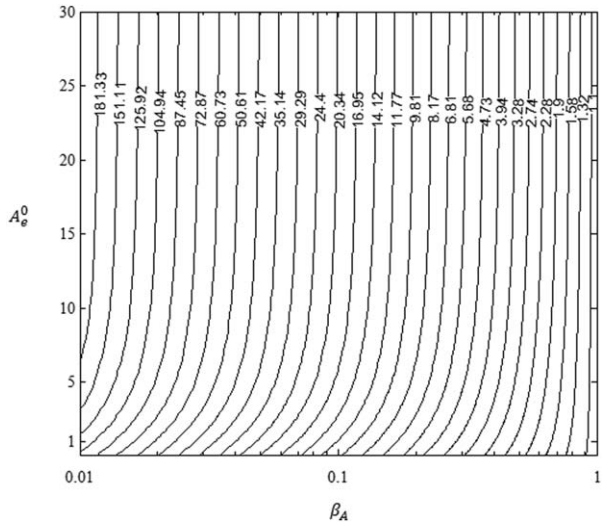

Figure 11. Iso-curves of the function $H^{0.95}$ for different absorbance values A_e^0 and competitive absorption factors β_A.

$$H^{0.95}(\beta_A, A_e^0) = \frac{\chi^{0.95}|_{\beta_A<1}}{\chi^{0.95}|_{\beta_A=1}} \tag{42}$$

The interest of this function is to be able to express the residence time $\tau^{0.95}$ for any values of β_A as a function of the residence time when there is no competitive absorption ($\beta_A = 1$). Indeed, at a given coefficient k (and thus at a given β_A), Eq. 42 can be transformed into

$$\left(\tau_s^{0.95}\right)_{\beta_A<1} = H^{0.95}(\beta_A, A_e^0) * \left(\tau_s^{0.95}\right)_{\beta_A=1} \tag{43}$$

Figure 11 presents the iso-curves of the function H for different absorbance values A_e^0 and competitive absorption factors β_A. When β_A decreases, the function H increases, meaning that the residence time required to reach a conversion of 95% should be increased if $\beta_A < 1$, when compared to the case where $\beta_A = 1$. This result is logical as, when the product B absorbs incident photons, the rate of conversion of the reactant A is slowed down. Figure 11 also shows that, at a given β_A, the function H slightly varies when $A_e^0 > 10$.

From this, by introducing a second ordinate axis in Figure 10, the variation of the residence time required to reach a conversion of 95%, when $\boldsymbol{\beta_A = 1}$ (noted $\left(\boldsymbol{\tau_s^{0.95}}\right)_{\boldsymbol{\beta_A=1}}$) as a function of the coefficient k for different absorbance and competitive absorption factors, can be represented. Note that $\left(\boldsymbol{\tau_s^{0.95}}\right)_{\boldsymbol{\beta_A=1}}$ is expressed in minutes. As mentioned previously, the values of $\left(\boldsymbol{\tau_s^{0.95}}\right)_{\boldsymbol{\beta_A=1}}$ do not vary significantly for strong absorbing media, explaining, thus, why the iso-curves of $\boldsymbol{A_e^0}$ are more and more close to each other. When $\boldsymbol{A_e^0 > 30}$, the value of $\left(\boldsymbol{\tau_s^{0.95}}\right)_{\boldsymbol{\beta_A=1}}$ can be determined from the straight line corresponding to $\boldsymbol{A_e^0 \geq 30}$. However, the values of $\left(\boldsymbol{\tau_s^{0.95}}\right)_{\boldsymbol{\beta_A=1}}$ are strongly dependent of the absorbances when these latter are low: the medium being transparent, it is necessary to increase the dose of photons required to reach a conversion of 95%, as discussed previously (Figure 3).

Once $\left(\tau_s^{0.95}\right)_{\beta_A=1}$ is graphically determined, the residence time required for a competitive absorption factor β_A, noted $\left(\tau_s^{0.95}\right)_{\beta_A<1}$, can be deduced from Eq. 43 and Figure 11.

To illustrate how Figure 10 should be used, the following parameters are considered

$$\begin{cases} W=1 \text{ mm} \\ \upsilon=1 \text{ (illuminated from both side)} \\ C_{A0}=10 \text{ mol.m}^{-3}=10^{-8} \text{ mol.mm}^{-3} \\ A_e^0=10 \\ \beta_A=0.5 \\ \Phi=1 \end{cases} \quad (44)$$

Using these parameters, the coefficient k can be determined by graphical reading (Figure 10B) or by using Eq. 41 (with $\beta_A=0.5$): a value of 0.12 min^{-1} is found. The maximum photon flux density received at the reactor wall, F_{wall}, is then calculated according to Eq. 39 and assuming a collimated beam ($\Lambda=1$): one finds $F_{wall}=$ 6 10^{-10} einstein mm^{-2} min^{-1} (namely 10^{-5} einstein m^{-2} s^{-1}). Subsequently, the residence time required to reach a conversion of 95% when $\beta_A=1$ is graphically determined from Figure 10C with $A_e^0=8$: one finds $\left(\tau^{0.95}\right)_{\beta_A=1}=9$ min. The latter residence time should be then corrected with the help of the function $H^{0.95}$ (Figure 11) to determine the real residence time. In this case, $H=2.74$ and $\left(\tau^{0.95}\right)_{\beta_A<1} \approx 25$ min. Thus, to avoid some diffusion limitations when operating the microreactor, the maximum photon flux density received at the reactor wall should be kept below 6 10^{-10} einstein mm^{-2} min^{-1}, and the residence time put equal to 25 min.

To conclude, this type of graphical representation (Figure 10) is an easy tool for determining the conditions (residence time and photon flux density received at the reactor wall) in which a microphotoreactor should work to avoid any diffusion limitations, and/or for knowing if, in the conditions in which a microphotoreactor operates, some diffusion limitations can exist.

Case study

Recent literature[7,18–20,45] shows that various types of photochemical reactions can be successfully performed in microreators. It is commonly admitted that, in addition to the usual advantages of the microspace, microreactors offer a better light control, thus leading to improve selectivity and yield of photochemical reactions. This section aims at showing, basing on a case study, that Figure 10 is an interesting tool able to give new insights on the advantages of microreactors for photochemistry.

For a photochemical reaction $A \xrightarrow{h\upsilon} B$ where A and B are in competition for absorbing incident photons, the effect of the decrease in microreactor width W is investigated in two cases: when C_{A0} is kept constant and when A_e^0 defined in Table 2 is kept constant. We consider that the microreactor width is two times smaller and that the same conditions as the ones described in Eq. 44 apply.

*Case n°1 (**$C_{A0}=cst$**).* In this case, the absorbance of the medium, A_e^0, is not conserved and a twofold reduction in the microreactor width W implies a twofold reduction in A_e^0. Considering the parameters defined in Eq. 44 with a width of 0.5 mm instead of 1 mm, A_e^0 becomes equal to 5. From Figure 10, the new coefficient k can be determined: it is found equal to 0.48 min^{-1}. The photon flux density at walls is thus calculated according to Eq. 39: one finds $F_{wall}=$ 1.2 10^{-9} einstein mm^{-2} min^{-1} (2 10^{-5} einstein m^{-2} s^{-1}), which is two times higher than the one obtained when $W=1$ mm.

Therefore, it is interesting to compare the productivity R^X (defined in Eq. 28) in both cases ($W=0.5$ and $W=1$ mm). For that, the photonic efficiency and the surface of the microreactor exposed to light should be taken into account. Considering an identical illuminated surface for both microreactors (S_{exposed}), the ratio of both productivities still depends on the photonic efficiency and on the photon flux density at walls. For the present example, according to Figure 4, the photonic efficiencies are determined: $(\eta^{0.95})_{W=1 \text{ mm}}=0.31$ and $(\eta^{0.95})_{W=0.5 \text{ mm}}=0.27$. Then, the productivities are compared

$$\frac{(R^{0.95})_{W=0.5\text{mm}}}{(R^{0.95})_{W=1\text{mm}}}=\frac{(F_{wall})_{W=0.5\text{mm}}}{(F_{wall})_{W=1\text{mm}}}\frac{(\eta^{0.95})_{W=0.5\text{mm}}}{(\eta^{0.95})_{W=1\text{mm}}} \approx 1,74 \quad (45)$$

Therefore, by having the microreactor width while avoiding diffusion limitations (i.e., with conserving $Da_{II}=1$), the productivity is increased by a factor equal to 1.74, as the photonic efficiency slightly decreases in a smaller microreactor (lower absorbance A_e^0).

*Case n°2 (**$A_e^0=cst$**).* In this case, the absorbance of the medium is kept constant by adjusting the concentration C_{A0}: a twofold reduction in the microreactor width leads then to a twofold increase in the concentration. Considering the parameters in Eq. 44 with a width of 0.5 mm instead of 1 mm, the coefficient k is still equal to 0.48 min^{-1} (β_A is unchanged). The photon flux density at the walls is then calculated from Eq. 39: the same value as for $C_{A0}=cst$ ($F_{wall}=$ 1.2 10^{-9} einstein mm^{-2} min^{-1}) is found. Again, it is interesting to look at the productivity. In this case, the photonic efficiency remains identical (0.31) as the absorbance is conserved. Therefore, for identical irradiated surfaces in the two microreactors, the comparison of the productivities leads to

$$\frac{(R^{0.95})_{W=0.5 \text{ mm}}}{(R^{0.95})_{W=1 \text{ mm}}}=\frac{(F_{wall})_{W=0.5 \text{ mm}}}{(F_{wall})_{W=1 \text{ mm}}}=2 \quad (46)$$

In the two cases discussed above, a reduction in microreactor width enables the productivity to be enhanced. Indeed, when decreasing W, the transverse diffusion time is increased ($t_d \propto W^2$), and thus the reaction time can be increased while avoiding some transverse diffusion limitations ($Da_{II} \leq 1$); for that,F_{wall} is increased, thus implying an increase in the productivity (Eq. 28). Note that the highest productivity is obtained when the absorbance of the medium (and not the initial concentration of the reactant A) is kept constant. Indeed, when $C_{A0}=cst$, the photonic efficiency decreases as the absorbance A_e^0 is lower.

Such enhanced productivities are the main reason why microphotoreactors are an advanced technology for photochemistry. Nevertheless, the present study also demonstrates the importance of the photonic efficiency. More generally, the energetic yield of the system has to be taken into account: such criteria include the photonic efficiency but also the design and the characteristics of the light sources.

Conclusion

To the authors' knowledge, this article presents for the first time a model aiming to predict the performances of a photochemical reaction at the exit of microphotoreactors. Some simplifying assumptions were made to make the present model easy to implement. From the numerical results obtained, the main following conclusions were formulated:

• the definition of the time characteristic of the photochemical reaction, τ_r, involved in both Da_I and Da_{II}, needed specific precaution;

• a quasi-complete conversion was reached at the outlet of the microreactor, whatever the absorbances A_e^0 and the competitive absorption factor β_A, when $1 \leq (1-e^{-\frac{A_e^0 \Lambda}{2}})\, Da_I \leq 2$;

• a diagram (Figure 2) linking the governing dimensionless numbers Da_I, Da_{II}, and Fo was established, enabling different operating zones to be identified;

• when the microreactor behaved as a PFR, for $\boldsymbol{A_e^0 \geq 5}$ Da_I (and thus the dose of photons) required to reach a conversion of 95 % became independent on the absorbance A_e^0, and was just specific to each value of β_A;

• when some transverse diffusion limitations existed, the conversion at the exit of the microreactor was significantly impacted, all the more than the competitive absorption factor β_A and the absorbance A_e^0 increased. This was due to the occurrence of strong transverse concentration gradients at the outlet of the microreactor.

From the necessity to avoid any diffusion limitations when operating in microreactors, a graphical methodology (Figure 10) was then proposed to determine the optimal operating conditions.

To conclude, the methodology proposed in this article enabled to formalize in a dimensionless way the problems associated to the implementation of photochemical reactions in microreactors. It, thus, constitutes a consistent basis for understanding and modeling the performances obtained, and also, for accompanying, either the transfer from conventional batch photoreactors to microreactors, or the scale-up from microreactors to advanced continuous photoreactors for industrial production.

In the future, the generic tools presented here will be applied for experimentally demonstrating the effect of Da_{II} on the conversion. To achieve this, a specific experimental setup will be constructed, and a photochemical reaction, where several species are in competition for absorbing photons, will be selected. In addition, some extensions to different photochemical reactions schemes and to different microreactor geometries will be implemented.

Notation

A_e^0 = Napierian absorbance (see Table 2)
$A_{e,A}^0$ = Napierian absorbance for the species A (see Table 2)
A_{Be}^0 = Napierian absorbance for the species B (see Table 2)
$\mathbf{C}$ = concentration matrix
C_A = concentration of the species A, mol m^{-3}
C_{A0} = concentration of the species A at the inlet of the microreactor, mol m^{-3}
C_{A^*} = concentration of the excited species A^*, mol m^{-3}
C_A^* = dimensionless concentration of the species A
C_B = concentration of the species B, mol m^{-3}
C_B^* = dimensionless concentration of the species B
Da_I = Damköhler one number defined in Table 3
Da_{II} = Damköhler two number defined in Table 3
D_m = molecular diffusion coefficient, m^2 s^{-1}
Dose = amount of photons received during the residence time by unit of reactor volume, einstein m^{-3}
e_i^a = local volumetric rate of photon absorption by compound i, einstein m^{-3} s^{-1}
e^{a*} = dimensionless total volumetric rate of photon absorption defined in Eq. SM.21
E_o = spherical irradiance, einstein m^{-2} s^{-1}
E^+ = spherical irradiance in the positive y-direction, einstein m^{-2} s^{-1}
E^- = spherical irradiance in the negative y-direction, einstein m^{-2} s^{-1}
E_+^* = dimensionless spherical irradiance in the positive y-direction
E_-^* = dimensionless spherical irradiance in the negative y-direction
$\mathbf{F}$ = photon flux density vector, einstein m^{-2} s^{-1}
f = photokinetic factor
k = coefficient defined in Eq. 39, s^{-1}
k_d = rate constant of the desactivation step $A^* \rightarrow A$, s^{-1}
k_R = rate constant of the reaction step $A^* \rightarrow B$, s^{-1}
Fo = Fourier number defined in Table 3
F_{wall} = photon flux density received at the wall of the microreactor, einstein m^{-2} s^{-1}
H = corrective function defined in Eq. 43
L = photon radiance, einstein m^{-2} sr^{-1}
L_c = length of the reactor, m
$\mathbf{M}$ = kinetics parameters matrix
n_r = number of moles of the molecule B produced, mol
q_P = photon flux received in the microreactor, einstein s^{-1}
$\mathbf{R}$ = reaction rate matrix
R^X = productivity defined at a given conversion defined, mol s^{-1}
r = reaction rate, mol m^{-3} s^{-1}
S_{exposed} = surface of the reactor exposed to the radiations, m^2
S = curvilinear coordinate of the light propagation, m
$\mathbf{u}$ = unit vector of light propagation
$\bar{u}$ = mean velocity in the microreactor, m s^{-1}
u_x = axial component of the velocity in the microreactor, m s^{-1}
V = Volume, m^3
W = microphotoreactor width, m
X = conversion
x = axial coordinate of the microreactor, m
x^* = dimensionless axial coordinate of the microreactor
y = transverse coordinate of the microreactor, m
y^* = dimensionless transverse coordinate of the microreactor

Greek letters

α = linear napierian absorption coefficient, m^{-1}
β_A = competitive absorbance factor defined with respect to the species A (see Table 2)
β_B = competitive absorbance factor defined with respect to the species B (see Table 2)
κ_A = molar napierian absorption coefficient of the species A, m^2 mol^{-1}
κ_B = molar napierian absorption coefficient of the species B, m^2 mol^{-1}
Λ = collimation factor
λ = wavelength, m
η^X = photonic efficiency at a given conversion defined, mol einstein^{-1}
Ω = solide angle, sr^{-1}
Γ = coefficient defined in Eq. 26
Φ = quantum yield, mol einstein^{-1}
φ = azimuthal angle, radian
υ = variable accounting for one or two sides illuminated
τ = residence time (s)
τ_d = time characteristic of the mass transfer by diffusion along the microreactor width, s
τ_r = time characteristic of the photochemical reaction, s
τ^X = residence time to reach a given conversion X, s
θ = zenith angle (radian) χ
χ = variable defined at a given conversion in Equations 38 and 39

Literature Cited

1. Hoffmann N. Photochemical reactions as key steps in organic synthesis. *Chem Rev*. 2008;108(3):1052–1103.
2. Pfoertner K-H, Oppenländer T. Photochemistry. In: *Ullmann's Encyclopedia of Industrial Chemistry*. Wiley-VCH Verlag GmbH & Co. KGaA; 2000.
3. Griesbeck A, Oelgemöller M, Ghetti F. *CRC Handbook of Organic Photochemistry and Photobiology*. Boca Raton, FL: CRC Press, 2012.
4. André MB, Maurette M-T, Oliveros E. *Technologie Photochimique*. Lausanne: Presses Polytechniques Romandes, 1986.
5. Braun AM, Peschl GH, Oliveros E. Industrial photochemistry. In: *CRC Handbook of Organic Photochemistry and Photobiology*. Boca Raton, FL: CRC Press, 2012:1.
6. Wörz O, Jäckel KP, Richter T, Wolf A. Microreactors, a new efficient tool for optimum reactor design. *Chem Eng Sci*. 2001;56(3): 1029–1033.

7. Oelgemöller M, Shvydkiv O. Recent advances in microflow photochemistry. *Molecules* 2011;16(12):7522–7550.
8. Elvira KS, i Solvas XC, Wootton RCR, deMello AJ. The past, present and potential for microfluidic reactor technology in chemical synthesis. *Nat Chem.* 2013;5(11):905–915.
9. Jähnisch K, Hessel V, Löwe H, Baerns M. Chemistry in Microstructured Reactors. *Angew Chem Int Ed.* 2004;43(4):406–446.
10. Coyle EE, Oelgemöller M. Micro-photochemistry: photochemistry in microstructured reactors. The new photochemistry of the future? *Photochem Photobiol Sci.* 2008;7(11):1313.
11. Su Y, Straathof NJW, Hessel V, Noël T. Photochemical transformations accelerated in continuous-flow reactors: basic concepts and applications. *Chem. Eur. J.* 2014;20:1–29.
12. Gorges R, Meyer S, Kreisel G. Photocatalysis in microreactors. *J Photochem Photobiol Chem.* 2004;167(2–3):95–99.
13. Visan A, Rafieian D, Ogieglo W, Lammertink RGH. Modeling intrinsic kinetics in immobilized photocatalytic microreactors. *Appl Catal B Environ.* 2014;150–151:93–100.
14. Matsushita Y, Ichimura T, Ohba N, Kumada S, Sakeda K, Suzuki T, Tanibata H, Murata T. Recent progress on photoreactions in microreactors. *Pure Appl Chem.* 2007;79(11).
15. Matsushita Y, Ohba N, Suzuki T, Ichimura T. N-Alkylation of amines by photocatalytic reaction in a microreaction system. *Catal Today* 2008;132(1–4):153–158.
16. Ueno K, Kitagawa F, Kitamura N. Photocyanation of pyrene across an oil/water interface in a polymer microchannel chip. *Lab Chip* 2002;2(4):231.
17. Wootton RCR, Fortt R, de Mello AJ. A microfabricated nanoreactor for safe, continuous generation and use of singlet oxygen. *Org Process Res Dev.* 2002;6(2):187–189.
18. Lainchbury MD, Medley MI, Taylor PM, Hirst P, Dohle W, Booker-Milburn KI. A protecting group free synthesis of (±)-neostenine via the [5 + 2] photocycloaddition of maleimides. *J Org Chem.* 2008; 73(17):6497–6505.
19. Park CP, Maurya RA, Lee JH, Kim D-P. Efficient photosensitized oxygenations in phase contact enhanced microreactors. *Lab Chip* 2011;11(11):1941.
20. Shvydkiv O, Yavorskyy A, Tan SB, Nolan K, Hoffmann N, Youssef A, Oelgemöller M. Microphotochemistry: a reactor comparison study using the photosensitized addition of isopropanol to furanones as a model reaction. *Photochem Photobiol Sci.* 2011;10(9):1399.
21. Lévesque F, Seeberger PH. Highly efficient continuous flow reactions using singlet oxygen as a "green" reagent. *Org Lett.* 2011; 13(19):5008–5011.
22. Oelgemöller M, Hoffmann N, Shvydkiv O. From "lab & light on a chip" to parallel microflow photochemistry. *Aust J Chem.* 2014; 67(3):337–342.
23. Aillet T, Loubiere K, Dechy-Cabaret O, Prat L. Photochemical synthesis of a "cage" compound in a microreactor: rigorous comparison with a batch photoreactor. *Chem Eng Process Process Intensif.* 2013;64:38–47.
24. Aillet T, Loubiere K, Dechy-Cabaret O, Prat L. Accurate measurement of the photon flux received inside two continuous flow microphotoreactors by actinometry. *Int J Chem React Eng.* 2014;12(1).
25. Charles G, Roques-Carmes T, Becheikh N, Falk L, Commenge J-M, Corbel S. Determination of kinetic constants of a photocatalytic reaction in micro-channel reactors in the presence of mass-transfer limitation and axial dispersion. *J Photochem Photobiol Chem.* 2011; 223(2–3):202–211.
26. Corbel S, Becheikh N, Roques-Carmes T, Zahraa O. Mass transfer measurements and modeling in a microchannel photocatalytic reactor. *Chem Eng Res Des.* 2014;92(4):657–662.
27. Andre JC, Viriot ML, Saïd A. Industrial photochemistry XI: comparison between different types of photoreactors and selective filtering for monomolecular photoreactions. *J Photochem Photobiol Chem.* 1988;42(2–3):383–396.
28. Bouchy A, Andre JC, George E, Viriot ML. Industrial photochemistry XIII: determination of the most suitable irradiation conditions for molecular photoreactions. *J Photochem Photobiol Chem.* 1989;48(2–3):447–463.
29. Midoux N, Roizard C, Andre J-C. Industrial photochemistry XVII: macroscopic transport effects on the performance of photochemical reactors. *J Photochem Photobiol Chem.* 1991;58(1):71–97.
30. Cassano AE, Martin CA, Brandi RJ, Alfano OM. Photoreactor analysis and design: fundamentals and applications. *Ind Eng Chem Res.* 1995;34(7):2155–2201.
31. Alfano OM, Romero RL, Cassano AE. Radiation field modelling in photoreactors—I. *Homogeneous media. Chem Eng Sci.* 1986;41(3): 421–444.
32. Li Puma G, Yue PL. Modelling and design of thin-film slurry photocatalytic reactors for water purification. *Chem Eng Sci.* 2003;58(11): 2269–2281.
33. Mohajerani M, Mehrvar M, Ein-Mozaffari F. Photoreactor design and CFD modelling of a UV/H2O2 process for distillery wastewater treatment. *Can J Chem Eng.* 2012;90(3):719–729.
34. Mohajerani M, Mehrvar M, Ein-Mozaffari F. CFD modeling of metronidazole degradation in water by the UV/H2O2 process in single and multilamp photoreactors. *Ind Eng Chem Res.* 2010;49(11):5367–5382.
35. Elyasi S, Taghipour F. Performance evaluation of UV reactor using optical diagnostic techniques. *AIChE J.* 2011;57(1):208–217.
36. Cassano AE, Silveston PL, Smith JM. Photochemical reaction engineering. *Ind Eng Chem.* 1967;59(1):18–38.
37. Hook BDA, Dohle W, Hirst PR, Pickworth M, Berry MB, Booker-Milburn KI. A practical flow reactor for continuous organic photochemistry. *J Org Chem.* 2005;70(19):7558–7564.
38. Sugimoto A, Fukuyama T, Sumino Y, Takagi M, Ryu I. Microflow photo-radical reaction using a compact light source: application to the Barton reaction leading to a key intermediate for myriceric acid A. *Tetrahedron* 2009;65(8):1593–1598.
39. Schechter RS, Wissler EH. Photochemical reactions in an isothermal laminar-flow chemical reactor. *Appl Sci Res.* 1960;9(1):334–344.
40. Irazoqui HA, Cerdá J, Cassano AE. The radiation field for the point and line source approximations and the three-dimensional source models: applications to photoreactions. *Chem Eng J.* 1976;11(1):27–37.
41. Cornet J-F, Dussap CG, Gros J-B, Binois C, Lasseur C. A simplified monodimensional approach for modeling coupling between radiant light transfer and growth kinetics in photobioreactors. *Chem Eng Sci* 1995;50(9):1489–1500.
42. Schuster A. Radiation through a foggy atmosphere. *Astrophys J.* 1905;21(1):1–22.
43. Cornet J-F. Calculation of optimal design and ideal productivities of volumetrically lightened photobioreactors using the constructal approach. *Chem Eng Sci.* 2010;65(2):985–998.
44. Nagy KD, Shen B, Jamison TF, Jensen KF. Mixing and dispersion in small-scale flow systems. *Org Process Res Dev.* 2012;16(5):976–981.
45. Terao K, Nishiyama Y, Tanimoto H, Morimoto T, Oelgemöller M, Morimoto T. Diastereoselective [2+2] photocycloaddition of a chiral cyclohexenone with ethylene in a continuous flow microcapillary reactor. *J Flow Chem.* 2012;2(3):73–76.

Manuscript received May 9, 2014, and revision received Dec. 1, 2014.